

Towards Dynamic Urban Bike Usage Prediction for Station Network Reconfiguration

Xi Yang and Suining He
The University of Connecticut
Storrs, Connecticut
{xi.yang,suining.he}@uconn.edu

ABSTRACT

Bike sharing has become one of the major choices of transportation for residents in metropolitan cities worldwide. A station-based bike sharing system is usually operated in the way that a user picks up a bike from one station, and drops it off at another. Bike stations are, however, not static, as the bike stations are often reconfigured to accommodate changing demands or city urbanization over time. One of the key operations is to evaluate candidate locations and install new stations to expand the bike sharing station network. Conventional practices have been studied to predict existing station usage, while evaluating new stations is highly challenging due to the lack of the historical bike usage.

To fill this gap, in this work we propose a novel and efficient bike station-level prediction algorithm called AtCoR, which can predict the bike usage at both existing and new stations (candidate locations during reconfiguration). In order to address the lack of historical data issues, virtual historical usage of new stations is generated according to their correlations with the surrounding existing stations, for AtCoR model initialization. We have designed novel station-centered heatmaps which characterize for each target station centered at the heatmap the trend that riders travel between it and the station's neighboring regions, enabling the model to capture the learnable features of the bike station network. The captured features are further applied to the prediction of bike usage for new stations. Our extensive experiment study on more than 23 million trips from three major bike sharing systems in US, including New York City, Chicago and Los Angeles, shows that AtCoR outperforms baselines and state-of-art models in prediction of both existing and future stations.

KEYWORDS

bike sharing, usage prediction, station-level, new stations, pick-ups and drop-offs, attention, spatio-temporal

1 INTRODUCTION

Thanks to mobile networking and location-based services, bike sharing has become one of the major transportation modalities for urban residents worldwide due to its convenience and efficiency. As a representative product of the sharing economy, it is often hailed as the excellent helper to solve the "last mile" problem in citizen transportation. Given the social and business importance, the bike sharing market is estimated to hit US\$5 billion by 2025¹.

A station-based bike sharing system (each station is equipped with multiple docks for bike parking) is usually operated in the way

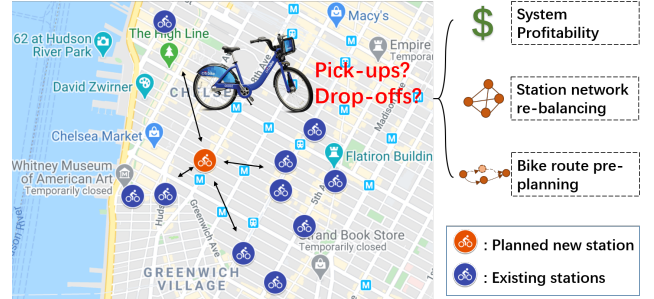


Figure 1: Illustration of bike sharing system and new station usage prediction.

that a user or rider picks up a bike from one station (pick-ups) and drops it off at another (drop-offs). All the resultant bike trips (usage that consists of pairs of pick-ups and drop-offs) connect different parts of the city, forming the *bike sharing station network*. The bike stations are, however, not static, as the bike sharing operators often *reconfigure* the stations to accommodate changing demands or city urbanization over time [8, 19], where a key operation is to evaluate candidate locations and then install new stations to expand the bike sharing station network [21, 34] as shown in Figure 1. It is essential for the operators to know the potential bike usage of a future station at a certain candidate location beforehand, which helps predicting the station profitability as well as its positive/negative effect upon the local mobility and traffic networks, enhancing the bike sharing service quality to the local community. This further benefits the future bike sharing network operations, including station re-balancing [14, 20, 26, 27, 31] and bike route pre-planning [35].

Despite the business and social importance, predicting bike usage at future stations is extremely challenging due to the lack of historical bike usage data of those stations. Conventional practices include user survey, crowdsourced feedbacks and public hearing, investigating the local demands, which is often costly and time-consuming. Operating regulations are also provided for bike sharing operators as guidance on candidate station locations, which is based primarily on geo-information such as distance to road intersections/public transit stations and station network density². However, such guidance is often too general to take into account uniqueness of different cities, causing inefficiency in station reconfiguration as well as reduced service quality and profit loss. While most of the existing studies focus on predicting the bike usage at the existing stations, only a few of them have comprehensively explored how to forecast new stations for the station reconfiguration purposes.

¹<https://www.globenewswire.com/news-release/2019/12/03/1955257/0/en/Bike-Sharing-Market-is-Predicted-to-Hit-5-Billion-by-2025-P-S-Intelligence.html>

²<https://www.transformative-mobility.org/assets/publications/The-Bikeshare-Planning-Guide-ITDP-Datei.pdf>

To fill this gap, in this work we propose a novel bike station prediction algorithm called AtCoR, based on Attention Convolutional Recurrent Neural Network, for predicting station-based bike usage of future stations. To tackle the lack of historical data issues for future/new stations to be deployed, virtual historical usage of new stations is generated according to their correlation with the surrounding existing stations. To predict the usage of new bike stations for reconfiguration decisions, we have designed novel station-centered heatmaps which characterize for each target station centered at the heatmap the trend that riders travel between it and the neighboring regions, so that the model is able to capture the learnable common patterns of the bike station network through a convolutional neural network (CNN). A Long Short-Term Memory (LSTM) neural network with temporal attention mask leverages the common patterns with integration of historical data and external factors, such as weekends, holidays, and weather, to predict the bike usage for existing stations. The captured bike usage features are then used to predict the pick-ups and drop-offs for new stations along with the virtual historical usage. An overview of information flow of this work is illustrated in Figure 2, summarizing the above process.

Our main technical contributions are as follows:

- 1) *Comprehensive bike data analysis for station prediction designs*: We have conducted comprehensive and detailed real-world data analysis on how the weather conditions, regional bike usage and surrounding POIs impact the bike usage in the metropolitan area like New York City (NYC), Chicago and Los Angeles (LA), and visualized them to validate our design insights for station reconfiguration prediction. These features serve as the shared patterns leveraged for the bike usage prediction, including predicting for the new stations.
- 2) *Dynamic urban bike usage prediction for reconfigured station networks*: We have designed a novel scheme called AtCoR to predict the station-level bike usage for new/future stations (candidate locations for reconfiguration) as well as existing/fixed ones. We propose a novel design of station-centered feature heatmap representation as an input of AtCoR, which calculates the differences between the features at the location of each station and those at the surrounding areas. The heatmaps account for the trend that riders travel from the center station to the neighborhood. The inclusion of the heatmaps significantly improves the accuracy of usage predictions. Heatmaps are then fed to AtCoR which consists of a deep Convolutional Neural Network (CNN) and a Long Short-Term Memory (LSTM) network with integration of temporal attention mechanism.
- 3) *Extensive experimental studies with real-world datasets*: We have conducted extensive experimental studies upon 23,955,989 trips in total, across three major bike sharing systems in the United States: 20,551,697 from Citi Bike in New York City (NYC), 3,113,950 from Divvy in Chicago, and 290,342 from Metro Bike in Los Angeles (LA). Our experimental studies, upon both the existing and new stations in the bike station network reconfiguration, have validated that AtCoR outperforms the other baseline models in multi-station predictions, often by more than 20% error reduction.

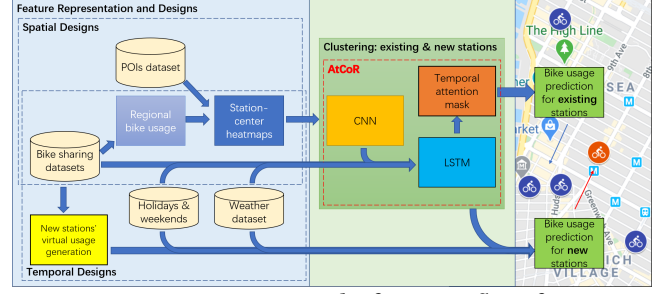


Figure 2: System overview and information flow of AtCoR.

While our studies focus on station-based bike sharing, the model and algorithm derived can be further extended to other transportation platform with deployment and expansion operations, including ride/car sharing [3, 9, 15] and scooter sharing [11].

The rest of the paper is organized as follows. We first conduct a brief survey on related studies in Section 2. Then we analyze the datasets, and find out the features and their corresponding representations for model input Section 3. Then the model is further presented in Section 4. Afterwards, we present our extensive experimental studies to evaluate the performance of AtCoR for both existing and new stations in Section 5. We will discuss the deployment in Section 6, and conclude in Section 7.

2 RELATED WORK

Traffic flow prediction has been studied recently due to the advances of intelligent transportation and smart cities. Gong et al. proposed a potential passenger flow predictor to help the decision on the places to construct new metro station [7]. Tang et al. tackled the dense and incomplete trajectories for citywide traffic volume inference [30]. For dockless bike sharing system, the potential bike distribution and the detection of parking hotspots in a new city has been made by Liu et al. [22, 23]. Different from above works on dockless bike sharing, we focus on station-based deployment due to its wider social acceptance, and our studies provide highly comprehensive studies of predicting usage for new/future stations before the bike sharing station reconfiguration [8].

Based on bike usage prediction granularity, there are three categories of prediction models in current works in the bike sharing systems: *city-level*, *cluster-level*, and *station-level* [17]. In *city-level* prediction, the aim is to predict bike usage for a whole city, while at the *cluster* level the goal is to predict bike usage for clusters of bike stations. The station cluster is generated by clustering algorithms such as the Bipartite Station Clustering [16], the Community Detection and the Agglomerative Hierarchical Clustering method [36], the K-means clustering and the Latent Dirichlet Allocation (LDA). Chen et al. further considered clusters as dynamic rather than static [2]. While city-level and cluster-level predictions save the computational cost by simplifying the problems, station-level [1, 4, 12, 14] prediction still benefits the bike sharing system management the most, including fine-grained station rebalancing, but yet is challenging.

Recent research efforts have also been made upon traffic prediction beyond the bike sharing systems. Deep learning approaches have been studied for traffic flow prediction [6, 10, 11, 13, 24, 33]. Yao et al. proposed a CNN-LSTM based transfer learning method to predict traffic flows across different cities [32]. Pan et al. used a

Table 1: List of symbols and definitions

Symbols	Definitions
n	New stations
f	Existing stations
F	Set of existing stations
j, k	Index of the stations
T, S	Ranges of timestamps
t, τ	Indices of timestamps
\mathcal{T}	Number of timestamps
g_{lat}, g_{lon}	Height and width of each grid
$\mathcal{G}_{lat}, \mathcal{G}_{lon}, \mathcal{P}$	Dimensions of station-centered heatmaps
H	Station-centered heatmaps
e	Entries of station-centered heatmaps
L	Station usage
h, w, c	Parameters of the convolutional layers
x	Input of LSTM
h	LSTM hidden state
c	LSTM cell state
d	Number of hidden units of LSTM
v, W, U, b	Trainable parameters
λ, γ	Attention scores between a pair of states
d	Decoder's input
ex	External features
ω	Similarity scores between a new station and its surrounding existing peers

deep meta learning model to predict urban traffic [29]. Ma et al. constructed spatial-temporal graphs of urban traffic which was learned by a deep convolutional neural network [25]. In this work, we study a novel approach based on deep learning designs and data-driven studies to handle the new stations usage prediction problems. Specifically, we propose a novel approach AtCoR which consists of a CNN component for modeling spatial characteristics and a LSTM with integration of a temporal attention mechanism for capturing temporal characteristics.

3 DATA ANALYSIS & FEATURE DESIGNS

Because no historical usage data of new stations is available, future mobility patterns might only be predicted through accessible spatial and temporal characteristics of the stations. In this work, we propose using station specific regional usage, points of interest (POIs), weather conditions and holidays as input features as they are all available once the locations and launching time of new stations are provided by system operators.

In this section, we first present the preliminary concepts defined for the feature designs of bike sharing stations in Section 3.1. Then in Section 3.2 we discuss our representation design of the features we choose, namely *station-centered heatmaps*, which significantly improve the model performance. We further cluster station networks based on such heatmaps to save computational cost of training.

Table 1 summarizes all the symbols as well as their definitions in this work.

3.1 Preliminary for Station Feature Studies

3.1.1 Overview of Datasets and New/Existing Stations. We conduct our data analytics upon three datasets: Citi Bike of NYC³ of 2019

³<https://www.citibikenyc.com/>

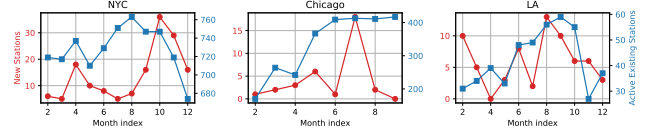


Figure 3: The number of active existing stations and new stations per month in NYC, Chicago and LA.

(20,551,697 trips), Divvy Bike of Chicago⁴ of the first three quarters of 2019 (3,113,950 trips), and Metro Bike of Los Angeles⁵ of 2019 (3,113,950 trips).

In this study, the *new stations* established in a set of certain time intervals $[T, T']$ are defined as the ones that have no historical bike usage data in the past 30 days, i.e. from $(T/24 - 30)$ days to T considering T on hourly basis, while the *active existing stations* (or existing stations in short) in a certain time interval $[S, S']$ are defined as the ones that have historical usage data every day in this time interval. Note that active existing stations focus on the existing stations which are populous with everyday bike usage.

For example, there are 454 active existing stations at the New York City (NYC) in 2019 in total, and from April 11, 2019 to July 19, 2019 there are 631 existing stations, while in June 2019 there are 8 new stations established, compared to totally 1,047 unique bike station coordinates in the whole year including those stations that are newly installed, removed, and relocated. The monthly number of active existing stations and new stations are shown in Figure 3 for the three datasets as demonstration.

We select the following spatial and temporal features in our modeling: regional usage in areas where bike stations are located, points of interest, weather conditions and holidays and weekends. Since there is no historical bike usage at the future locations of the new bike stations, it is difficult to directly characterize the mobility patterns for the target locations. However, the mobility patterns are strongly related to the spatial and temporal features of those locations. Thus, in this work AtCoR incorporates the correlations with the above features for the new station prediction.

3.1.2 Regional Usage. To characterize the urban bike usage in a computationally efficient manner, we discretize the neighborhood city map around each station into grids, each of which is an g_{lat} m \times g_{lon} m rectangular region. The total bike pick-ups/drop-offs within the grid can represent the bike usage popularity of this specific region. Bikes rented at the popular regions tend to be returned at surrounding regions. Therefore, the station-centered regional usage distribution is chosen an essential input feature.

3.1.3 Points of Interest (POIs). Another key insight of feature selection is that the differences in the POI distributions around each station can steer the bike riders' travels with the corresponding preferences or purposes. Therefore, the POI distributions are used as another important features. Following the manners of defining regional station usage, the POI distributions are defined as the total numbers of POIs within a g_{lat} m \times g_{lon} m grid for each POI category.

⁴<https://data.cityofchicago.org/Transportation/Divvy-Trips/fg6s-gzvz>

⁵<https://bikeshare.metro.net/>

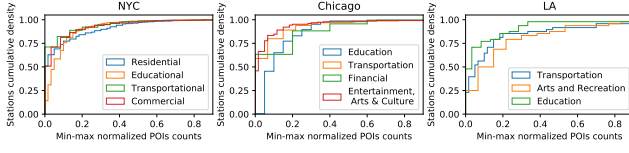


Figure 4: POIs distributions around bike stations in NYC, Chicago and LA.

Figure 4 illustrates some examples of the different distributions of different categories of POIs in a $500m \times 500m$ grid region. POIs around active existing stations from April 11, 2019 to July 19, 2019 are shown here with the numbers of POIs normalized by the min-max method.

Specifically, the POIs data of NYC are obtained through NYC Open Data⁶ which contain 13 major categories, such as residential, education facility, cultural facility, recreational facility, social services, transportation facility, commercial, government facility (non public safety), religious institution, health services, public safety, water and others. The POIs of Chicago are obtained through OpenStreetMap Overpass API⁷ where POIs are categorized by the OSM tag of amenity including sustenance, education, transportation, financial, healthcare, entertainment, arts & culture, and others. The POIs of LA are obtained through LAC Open Data⁸ which include communications, transportation, private industry, health and mental health, social services, postal, arts and recreation, community groups, municipal services, public safety, education, government, emergency response, physical features and environment.

3.1.4 Weather Conditions, Holidays and Weekends. The station usage is highly correlated with the weather conditions. We have collected and analyzed the weather condition data from open source weather data API⁹. We have analyzed the correlations between weather conditions and the station usage. Analysis of one-year bike usage reveals that both high and low temperature decreases the bike usage. The effect of daily temperature, precipitation and wind speed on daily overall usage of the city is illustrated in Figures 5 and 6. Clearly, precipitation, including rain, snow and large wind speed, significantly reduces the bike usage. Given above, the weather conditions including temperature, precipitation and wind speed are chosen as the input features. Besides weather conditions, the bike usage has different patterns on federal holidays and weekends from that on workdays. Specifically, we set the indicator as 1 if a time interval belongs to holiday/weekend periods, or 0 for weekdays otherwise. As an example, for the time interval of [0:00 a.m., 1:00 a.m.], 2019-01-01, the external vector including temperature, wind speed, precipitation and holiday/weekends, is given by [47 °F, 1.5 mph, 0.08 in, 1].

3.2 Feature Representations & Designs

Given the spatial and temporal features presented above for each station, we present a representation design to integrate them as the model inputs, which will be discussed in details as followed.

⁶<https://data.cityofnewyork.us/City-Government/Points-Of-Interest/rxuy-2muj>

⁷https://wiki.openstreetmap.org/wiki/Overpass_API

⁸<https://data.lacounty.gov/>

⁹<https://api.weather.com>

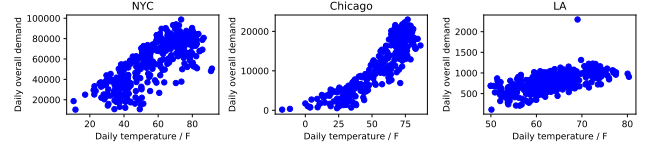


Figure 5: Temperature effect on daily overall bike usage.

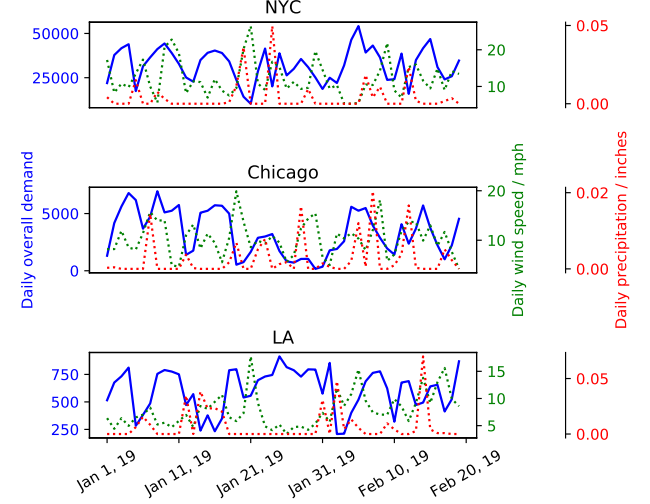


Figure 6: The effect of precipitation and wind speed on city's daily overall bike usage.

3.2.1 Station-centered Heatmaps. We construct a $\mathcal{G}_{lat} \times \mathcal{G}_{lon} \times \mathcal{P}$ heatmap centered at the stations studied where each grid is a g_{lat} m $\times g_{lon}$ m area on city map with \mathcal{P} channels including the regional usage and POIs distribution of the grid area. The first two channels of the heatmap are the regional pick-ups and drop-offs, respectively, with each of the following channel as the POIs distributions of one POIs category. Every entry of the heatmaps is the regional usage or the POIs amount for the corresponding grid location. Figure 7 shows a 11×11 regional pick-ups as the first channel of the station-centered heatmap for a candidate station in NYC.

After construction of the heatmaps centered at a particular station, the heatmaps are normalized by subtracting each one of the $\mathcal{G}_{lat} \times \mathcal{G}_{lon}$ grid features by the features of the center grid. This way, the normalized heatmaps represent the riders' motivations or mobility trends departing from this station to the neighborhoods, characterizing the spatial-temporal features near a station.

3.2.2 Station Clustering. To enhance the learning efficiency upon large-scale bike station network, we design a clustering scheme for the bike stations and train the AtCoR for certain cluster. We cluster existing stations and newly established ones all together. This way, we can save computational cost by reducing the amount of stations being trained, while the predictions upon new stations can be enabled by the patterns learned from other stations.

We adopt the K-means clustering algorithm to find out the clusters from the normalized station-centered heatmaps constructed as in Section 3.2. We first calculate the sum of all the $\mathcal{G}_{lat} \times \mathcal{G}_{lon}$

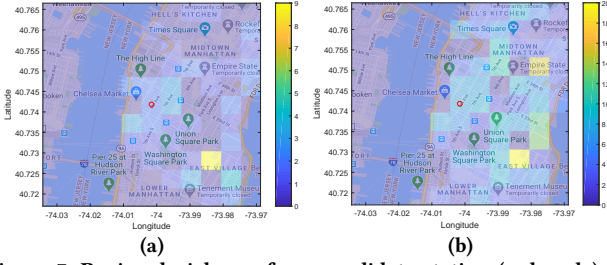


Figure 7: Regional pick-ups for a candidate station (red cycle) in Manhattan, NYC on (a) Sunday 01-20-2019 from 8:00 a.m. to 9:00 a.m.; (b) Monday 01-21-2019 from 8:00 a.m. to 9:00 a.m.

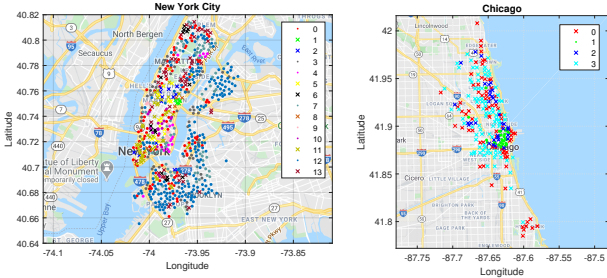


Figure 8: The cluster results of existing and new stations. The clusters represented by dots contain new stations, while the cross ones have only existing stations.

entries at each channel, and the mean of heatmaps over the time-frame $[T, T']$, generating vectors of length \mathcal{P} . The POI metric scores between the heatmaps of stations j and k for the clustering are calculated from the Euclidean distance between the generated vector:

$$Sim_{j,k} = \left\| \sum_{e=1}^{G_{lat} \times G_{lon}} \bar{H}_j^e - \sum_{e=1}^{G_{lat} \times G_{lon}} \bar{H}_k^e \right\|. \quad (1)$$

The combination of both existing and new stations in each city are then clustered based on the above metric scores. The results of clustering existing and new stations for NYC and Chicago based on $11 \times 11 \times \mathcal{P}$ heatmaps are shown below on Figure 8.

4 ATCOR: USAGE PREDICTION FOR STATION NETWORK RECONFIGURATION

We further discuss the details of AtCoR model in this section. We first define our usage problem, followed by a description of model structure in Section 4.1. Our model is trained on the datasets of active existing stations, and the details will be discussed in Section 4.2.

4.1 Problem & Model Definitions

4.1.1 Problem Definition. The problem in this study can be defined as: given the input station-centered heatmaps, $\mathbf{H}_{n,\tau'}$, and the external features $\mathbf{ex}_{\tau'}$, including the weather conditions and weekend/holidays information, for each station n at the period of time $\tau' \in [1, \mathcal{T}]$, either an existing or new one after reconfiguration, predict future usage (pick-ups and drop-offs), $L_{n,\tau}$, where $\tau = \mathcal{T} + 1$ is the target time interval for an existing station or the one when the new station is established after reconfiguration.

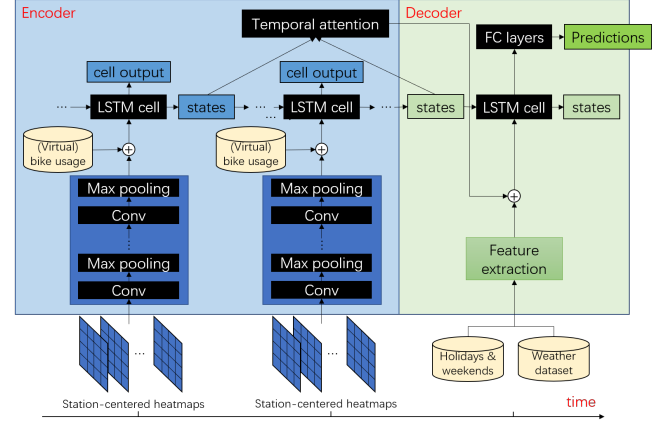


Figure 9: Illustration of model designs in AtCoR.

4.1.2 Model Overview. Our model consists of three major modules.

- 1) *Spatial feature learning*: A deep-channel CNN learns the station specific heatmaps which describe the driving force of usage for each particular station based on its spatial characteristics.
- 2) *Temporal feature learning*: The output of CNN combined with historical usage data is then fed as input of a LSTM which learns the temporal pattern of station's usage.
- 3) *Feature attention characterization*: A temporal attention mechanism is applied to further capture and differentiate the correlations between features across different timestamps.

An overview of AtCoR is further illustrated in Figure 9. The details of each module will be presented as follows.

4.1.3 Convolutional Neural Network (CNN). As described before, the station-specific or station-centered heatmaps as the representation of spatial features, i.e. the POIs distribution and regional usage popularity, indicate the motivation of people heading to places around and hence correlate with the bike usage. Differences in this driving force may result in different directions of bike usage and are represented by the designed heatmaps. However, the mechanism behind this driving force of bike usage can be too complicated to formulate, and simple vector concatenation is not enough. Therefore, we propose a deep-channel CNN model to learn the correlation between station specific spatial features in an area and station bike usage. Note that different from previous studies [25], we focus on learning station-centered heatmaps to further identify the useful correlations between the center station's usage and the neighborhood.

The CNN has C convolutional layers, each of which is followed by a max pooling layers. The size of the convolutional layers are $h \times w \times c$, all with `relu` activation function. A fully connected layer is implemented as the last layer to generate the output of CNN of size 1.

4.1.4 Long Short-Term Memory (LSTM). The output of the CNN is concatenated with historical usage data as the input of LSTM. The last hidden state of the LSTM cell is connected to a fully connected layer to generate predictions. The equations of an LSTM cell at

timestamp t are listed below:

$$\begin{aligned}
 \mathbf{i}_t &= \sigma \left(\mathbf{W}^i [\mathbf{h}_{t-1}, \mathbf{x}_t] + \mathbf{b}^i \right), \\
 \mathbf{f}_t &= \sigma \left(\mathbf{W}^f [\mathbf{h}_{t-1}, \mathbf{x}_t] + \mathbf{b}^f \right), \\
 \mathbf{o}_t &= \sigma \left(\mathbf{W}^o [\mathbf{h}_{t-1}, \mathbf{x}_t] + \mathbf{b}^o \right), \\
 \tilde{\mathbf{c}}_t &= \tanh \left(\mathbf{W}^c [\mathbf{h}_{t-1}, \mathbf{x}_t] + \mathbf{b}^c \right), \\
 \mathbf{c}_t &= (\mathbf{f}_t * \mathbf{c}_{t-1} + \mathbf{i}_t * \tilde{\mathbf{c}}_t), \\
 \mathbf{h}_t &= \tanh(\mathbf{c}_t) * \mathbf{o}_t,
 \end{aligned} \tag{2}$$

where $\mathbf{x}_t \in \mathbb{R}^l$ is the input of this timestamp of size l , which is the concatenation of historical usage and the CNN output, \mathbf{c}_t and \mathbf{h}_t are the cell state and hidden state of LSTM cell at time t , \mathbf{i}_t , \mathbf{f}_t , \mathbf{o}_t and $\tilde{\mathbf{c}}_t$ are intermediate variables of LSTM cell, and $\mathbf{W}^q \in \mathbb{R}^{d \times (d+l)}$ and $\mathbf{b}^q \in \mathbb{R}^d$ where $q = i, f, o$ are trainable variables, and d is the number of hidden units of LSTM cell.

4.1.5 Temporal Attention. The temporal attention mechanism captures correlation between features across different timestamps. The intuition behind this is that there is a strong temporal dependency of the usage of a station at time t , for example, on the usage at the same time one day ago. The temporal attention scores between the current decoder LSTM timestep t and one of the previous encoder LSTM hidden states, $\lambda_{t,t'}$, are calculated as Eq. (3) by a concatenation manner:

$$\lambda_{t,t'} = \mathbf{v}_a^T \tanh(\mathbf{W}_a [\mathbf{h}_{t-1}; \mathbf{c}_{t-1}] + \mathbf{U}_a \mathbf{h}_{t'} + \mathbf{b}_a), \tag{3}$$

where $\mathbf{v}_a, \mathbf{b}_a \in \mathbb{R}^d$, $\mathbf{W}_a \in \mathbb{R}^{d \times 2d}$ and $\mathbf{U}_a \in \mathbb{R}^{d \times d}$ are learnable parameters, d is the number of hidden units of LSTM cell, \mathbf{h}_t and \mathbf{c}_t are hidden state and cell state of decoder at timestamp t , and $\mathbf{h}_{t'}$ is hidden state of encoder at timestamp t' , which is in range of $[1, \mathcal{T}]$. The attention weight, denoted as $\gamma_{t,t'}$, is then a softmax function of $\lambda_{t,t'}$ as in Eq. (4):

$$\gamma_{t,t'} = \frac{\exp(\lambda_{t,t'})}{\sum_{t'=1}^{\mathcal{T}} \exp(\lambda_{t,t'})}. \tag{4}$$

The weighted sum of the encoder LSTM hidden states, \mathbf{d}_t , shown in Eq. (5) concatenated with external features \mathbf{ext}_t , $[\mathbf{d}_t; \mathbf{ext}_t]$, serves as the input of decoder:

$$\mathbf{d}_t = \sum_{t'=1}^{\mathcal{T}} \gamma_{t,t'} \mathbf{h}_{t'}, \tag{5}$$

where \mathcal{T} is the number of encoder timestamps.

4.2 Model Training & Prediction for New Stations

As conventional practices, we handle the existing station prediction based on the historical data available. Given absence of historical data, the predictions of the usage for new stations are based on the model trained on the active existing stations. To address the initialization problem of the model, during the training process, we generate the virtual trip data based on the weighted average of those from multiple existing stations. This is achieved by randomly picking a batch from the samples of all the existing stations at each training epoch. This way, the model is able to learn their shared bike usage patterns across all the existing stations, and such knowledge

learned can be used to predict the usage of new stations, considering that the new stations share correlated spatial and temporal usage features of existing stations.

The model is trained upon the existing stations within each cluster. To address the model initialization without historical data, for the new stations we design an efficient mechanism to generate the virtual historical usage from those of surrounding existing stations. We note that the two adjacent stations have similar bike usage and mobility patterns because of their similar spatial-temporal characteristics. Therefore, we generate the virtual bike usage by the distances between stations. Specifically, we compute the geographic similarity score between a new station, n , and an existing peer in its neighborhood, f , based on their mutual geographic distance in km:

$$Sim_{n,f} = \frac{1}{\text{distance}(n, f)}. \tag{6}$$

Then the similarity scores across all the existing stations is normalized to find the weights for the known bike usage assigned upon each existing station:

$$\omega_{n,f} = \frac{Sim_{n,f}^2}{\sum_{f=1}^F Sim_{n,f}^2}. \tag{7}$$

The virtual bike usage for the new station at time τ based on the historical usage of those existing stations, $L_{f,\tau}$ is finally calculated by:

$$L_{n,\tau} = \sum_{f \in F} \omega_{n,f} L_{f,\tau}, \tag{8}$$

where F is the set of existing stations.

5 EXPERIMENTAL STUDIES

In this section, we present the experimental results based on the datasets of Citi (NYC), Divvy (Chicago) and Metro (LA). The experimental settings are first introduced in Section 5.1, followed by experimental results on existing/new stations in Section 5.2.

5.1 Experimental Settings

We compare AtCoR with the following baselines and state-of-art models on the given datasets:

- (1) *ARIMA*: Auto Regressive Integrated Moving Average for time-series forecasting. The size of sliding window is set to be 24.
- (2) *RNN*: Simple Recurrent Neural Network for time-series predictions [28]. The length of input sequence is 24.
- (3) *LSTM*: Long Short-Term Memory neural network [18] predicts future usage with historical data of last 24 hour.
- (4) *GRU*: Gated Recurrent Units as another recurrent neural network for time-series predictions [5].
- (5) *GCN*: Graph Convolutional Neural Networks with Data-driven Graph Filter [1] predicts station-level usage taking into account of station correlations.

We are leveraging the features for previous 24 hours to predict the station-level bike usage for the next timestamp. For the evaluation of the existing stations for NYC and Chicago datasets, our model as well as comparison schemes are trained based on the hourly usage data from April 11, 2019 to July 19, 2019 (2,400 hours

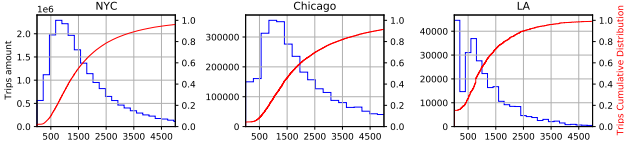


Figure 10: Distributions of bike trip distance (meters) for NYC, Chicago and LA.

duration), and are tested on the hourly usage data from July 20, 2019 to August 18, 2019 (720 hours duration). For LA datasets, the models are trained based on the 4-hour bike usage data in June 2019 (720 hours duration), and are tested on the data for the following 30 days (720 hours duration).

For the evaluation of the new stations, we find out all the deployed stations from May to August 2019 for NYC and Chicago, and those from June to December 2019 for LA. Our model as well as the baselines are tested on the usage data within 4 weeks (672 hours duration) for NYC and Chicago and 2 weeks for LA from the first appearance of the hourly usage of the stations. The stations with sufficient bike usage are of our interest here, and we discard those with little usage (say, less than 10 pick-ups/drop-offs per day). For new stations in LA, due to the large sparsity in the bike usage data, we consider the appearance of consecutive bike usage as the first usage and the start of our evaluations. The numbers of existing/new stations studied in our experimental evaluations are further identified and listed as follows. The numbers of existing and new stations studied, (existing, new), for each city are as follows: (631, 15) for NYC, (229, 13) for Chicago, (48, 7) for LA. The existing and new stations are clustered together in the manner described in Section 3.2.2. We train AtCoR and baseline models on all the clusters of the three bike sharing systems. Then we evaluate models regarding their predictions of new stations.

Figure 10 shows that a majority of bikes rented at one station in NYC, Chicago and LA, are returned at stations beyond 500m away, demonstrating that for a specific station there is a small number ($< 20\%$) of bike transitions between the stations within a grid of $500\text{m} \times 500\text{m}$ and the bikes rented at this region are mostly returned to regions somewhere else. In addition, a majority of bike trips are within the range of 500m and 5,000m as shown in Figure 10. Therefore, the size of station-centered heatmaps discussed in Section 3.2.1 is set to be $11 \times 11 \times \mathcal{P}$, where \mathcal{P} is 2 (regional pick-ups and drop-offs) plus the total number of POIs categories (13 for NYC, 7 for Chicago and 15 for LA), and each grid of the heatmaps is a $500\text{m} \times 500\text{m}$ area on the city map. This way, the heatmaps cover most of the areas where the riders can reach by the bikes rented from the center station.

Other model parameters of AtCoR are set as followed. The CNN component has 3 layers convolutional layers with sizes $h \times w \times c$; we set $3 \times 3 \times 256$, $3 \times 3 \times 128$ and $2 \times 2 \times 64$, respectively, and relu activation function for each of them. Each of the first two convolutional layers is followed by a maxpooling layer. The final convolutional layer is connected with a fully connected layer which converts the CNN’s output into the one of size 1. The number of layers of LSTM is 1,024. The dropout rate for the LSTM is 0.5. The learning rate is 0.001. The batch size is set to be 128. Total number of training epochs is 5,000. We have implemented AtCoR and other schemes in Python 3.7 and Tensorflow 2.1, and the models are

Table 2: Comparison between AtCoR and other baseline and state-of-art models for existing stations of the three datasets.

Schemes			ARIMA	RNN	GCN	LSTM	GRU	AtCoR
Citi	Pick-up	MAE	2.682	2.345	2.240	2.164	2.166	1.771
		MSE	30.028	18.711	12.226	16.080	16.143	10.599
	Drop-off	MAE	2.564	2.265	2.084	2.100	2.112	1.730
		MSE	24.762	16.514	11.318	14.210	14.245	9.447
Divvy	Pick-up	MAE	1.964	1.832	2.300	1.437	1.418	1.263
		MSE	23.693	14.866	6.382	11.293	10.732	7.687
	Drop-off	MAE	1.927	1.633	1.067	1.247	1.404	1.247
		MSE	21.075	13.584	6.382	10.937	10.508	7.980
Metro	Pick-up	MAE	2.126	3.258	1.276	1.878	1.936	1.462
		MSE	8.578	16.071	4.895	7.471	7.26	4.879
	Drop-off	MAE	2.154	1.478	1.480	1.251	1.005	1.435
		MSE	8.752	4.535	3.965	3.393	2.245	4.610

trained and evaluated upon a desktop server with Intel i5-8700K, 16GB RAM, Nvidia GTX 1060/1050Ti and Windows 10.

We use mean square error (MSE) as the training metric, and we evaluate model performance as well as the results based on both MSE and mean absolute error (MAE):

$$MSE = \frac{1}{M} \sum_i (y_i - \hat{y}_i)^2, \quad MAE = \frac{1}{M} \sum_i |y_i - \hat{y}_i|, \quad (9)$$

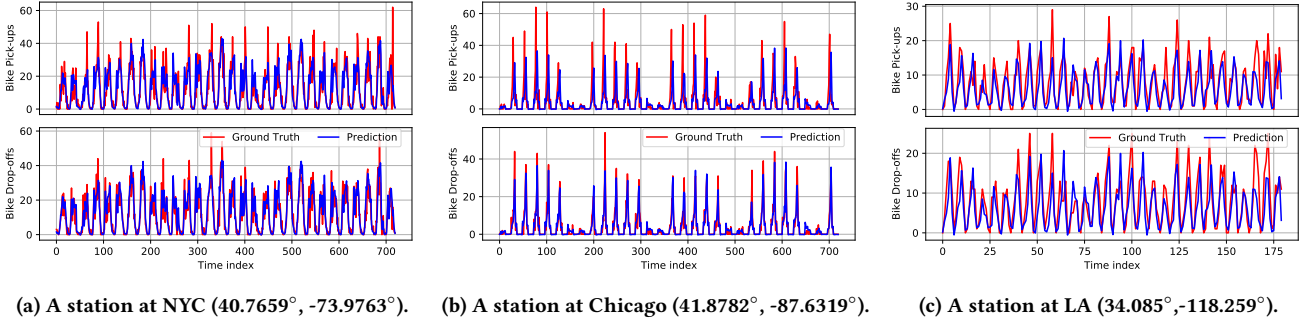
where M , y_i and \hat{y}_i are the total number of predictions made by the evaluated model, the ground-truth of the bike usage and the predicted bike usage, respectively.

5.2 Experimental Results

5.2.1 Usage Prediction for Existing Stations. First, we test our model on all active existing stations for all three datasets. The accuracy of bike usage predictions across the existing stations is shown in Table 2. It is shown that our model achieves overall better accuracy compared with other baselines for the systems in NYC, Chicago and LA. It is mainly because the station-centered heatmaps incorporate the trend that the bike riders travel between the stations. Focusing upon each station’s neighborhood, a heatmap characterizes the mobility patterns, which are learned and captured by AtCoR, and thus the bike usage at the new stations with similar neighborhood patterns can be further predicted. For Metro in LA, GCN achieves comparable or slightly better performance like AtCoR, likely due to the sparsity of bike station network in LA. Despite this, AtCoR has shown high accuracy and robustness with complicated mobility patterns.

Figure 11 illustrates the bike usage (pick-ups and drop-offs) predictions for the three existing stations in NYC, Chicago and LA. We can observe that the predictions of AtCoR are highly accurate, and close to the ground-truth measurements. Such accuracy can enable advanced bike station operational applications like station demand and supply rebalancing.

5.2.2 Bike Usage Prediction for New Stations. The predictions of bike usage for new stations can be done using the knowledge learned from the existing stations. Given the trained models from all the existing stations, RNN, LSTM and GRU can be directly applied to predict each individual new stations, and therefore we focus on comparing AtCoR with the three approaches here. We leverage the knowledge learned from the existing stations for the predictions of new stations given the bike station network reconfiguration. MAE



(a) A station at NYC (40.7659° , -73.9763°). (b) A station at Chicago (41.8782° , -87.6319°). (c) A station at LA (34.085° , -118.259°).

Figure 11: Hourly bike usage prediction for the existing stations in the three datasets.

Table 3: Performance comparison for predictions of new stations.

Schemes			RNN	LSTM	GRU	AtCoR
Citi	Pick-up	MAE	2.922	2.760	2.736	2.495
		MSE	20.961	18.652	18.461	15.883
	Drop-off	MAE	2.774	2.728	2.738	2.568
		MSE	17.833	18.930	19.016	15.835
Divvy	Pick-up	MAE	2.092	1.814	1.825	1.627
		MSE	23.475	21.089	21.025	13.282
	Drop-off	MAE	1.812	1.589	1.639	1.442
		MSE	14.126	11.491	12.317	8.223
Metro	Pick-up	MAE	1.552	1.249	1.246	1.098
		MSE	3.286	3.425	3.135	2.439
	Drop-off	MAE	1.588	1.583	1.216	1.043
		MSE	3.683	3.662	2.463	2.795

Table 4: Comparison of performance between AtCoR w/ and w/o virtual generated data.

Schemes		Citi		Divvy		Metro	
		MAE	MSE	MAE	MSE	MAE	MSE
Pick-up	AtCoR w/ virtual	2.384	15.018	1.638	11.983	1.305	4.639
	AtCoR w/o virtual	2.387	16.661	1.685	14.528	1.395	5.014
Drop-off	AtCoR w/ virtual	2.666	15.892	1.589	9.320	1.561	5.797
	AtCoR w/o virtual	2.547	16.510	1.522	10.300	1.727	7.929

and MSE of new stations' usage predictions, pick-ups and drop-offs, by AtCoR as well as three baselines, RNN, LSTM and GRU, are shown in Table 3. As is shown, AtCoR outperforms those three baseline models in predicting the usage of new stations for all three bike sharing systems.

We illustrate the performance with and without the virtual bike usage data generated. Virtual bike usage one day ahead of the first bike usage of new stations are generated as in Section 4.2 as the starting points. The virtual usage provides an initial inference for the models regarding how the mobility pattern of a new station possibly look like, enhancing the model accuracy as is shown in Table 4. Here we only compare the MAE and MSE for predicting the next 24 hours after the first use of the stations given the data availability.

6 DISCUSSION

Incorporating Other Information: Despite the features selected in this work as described in Section 3.1, other features may also be correlated with bike usage, such as events and demographic distributions [2]. However, such information is not considered due to the limit of our current resources. Our prediction accuracy could be further increased with the inclusion of those features in our model.

Nevertheless, the generic design of station-centered heatmaps as the feature representations in this study allows the easy integration of other information.

Sparsity of Usage Data: Though we focus on active existing stations in this study, a lot of stations are not so active that their bike usage is low, especially in LA. For experimental study of LA bike usage, we consider 4-hour time interval as one timestamp to lower the influence of data sparsity. Predicting the bike usage with sparsity is challenging, yet important for system management. Further study on how to deal with sparse historical data is necessary.

Similarity Scores for Virtual Data Generation: As mentioned in Section 5.2.2, virtual historical usage is essential for the first few predictions, and their accuracy depends on the quality of the initial inference in addition to the model performance. In this work, we compute the virtual historical usage based on the mutual geometric distances between stations, which has been shown to benefit predicting the new stations. However, further enhanced inference can be achieved by inclusion of other information such as crowd's awareness of new stations, where a comprehensive mechanism is needed for future study.

7 CONCLUSION

In this work, we propose a novel bike station prediction algorithm called AtCoR for predicting station-based bike usage of future stations given bike station network reconfiguration. We design novel station-centered heatmaps which characterize for each target station centered at the heatmap the trend that the riders travel between it and the neighboring regions, making the common patterns of the bike station network learnable. AtCoR further leverages such knowledge learned to predict the usage for new stations with the aid of virtual historical usage of new stations generated according to their correlation to the surrounding existing stations. Extensive experiment study on the bike sharing systems of NYC, Chicago and LA shows AtCoR is capable in predicting usage at new/future stations as well as existing stations, and outperforms the baseline and state-of-art models in our experimental evaluations.

REFERENCES

- [1] Di Chai, Leye Wang, and Qiang Yang. 2018. Bike flow prediction with multi-graph convolutional networks. In *Proc. ACM SIGSPATIAL*. 397–400.
- [2] Longbiao Chen, Daqing Zhang, Leye Wang, Dingqi Yang, Xiaojuan Ma, Shijian Li, Zhaohui Wu, Gang Pan, Thi-Mai-Trang Nguyen, and Jérémie Jakubowicz. 2016. Dynamic cluster-based over-demand prediction in bike sharing systems. In *Proc. ACM UbiComp*. 841–852.
- [3] Min Hao Chen, Abhinav Jauhri, and John Paul Shen. 2017. Data driven analysis of the potentials of dynamic ride pooling. In *Proc. ACM SIGSPATIAL*. 7–12.
- [4] Po-Chuan Chen, He-Yen Hsieh, Kuan-Wu Su, Xanno Kharis Sigalingging, Yan-Ru Chen, and Jenq-Shiou Leu. 2020. Predicting station level demand in a bike-sharing system using recurrent neural networks. *IET Intelligent Transport Systems* (2020).
- [5] Kyunghyun Cho, Bart Van Merriënboer, Dzmitry Bahdanau, and Yoshua Bengio. 2014. On the properties of neural machine translation: Encoder-decoder approaches. *arXiv preprint arXiv:1409.1259* (2014).
- [6] Zubair Md Fadlullah, Fengxiao Tang, Bomin Mao, Nei Kato, Osamu Akashi, Takeru Inoue, and Kimihiro Mizutani. 2017. State-of-the-art deep learning: Evolving machine intelligence toward tomorrow's intelligent network traffic control systems. *IEEE COMST* 19, 4 (2017), 2432–2455.
- [7] Yongshun Gong, Zhibin Li, Jian Zhang, Wei Liu, and Jinfeng Yi. 2019. Potential Passenger Flow Prediction: A Novel Study for Urban Transportation Development. *arXiv preprint arXiv:1912.03440* (2019).
- [8] Suining He and Kang G Shin. 2018. (Re) Configuring Bike Station Network via Crowdsourced Information Fusion and Joint Optimization. In *Proc. ACM MobiHoc*. 1–10.
- [9] Suining He and Kang G. Shin. 2019. Spatio-Temporal Adaptive Pricing for Balancing Mobility-on-Demand Networks. *ACM Trans. Intell. Syst. Technol.* 10, 4, Article 39 (July 2019), 28 pages.
- [10] Suining He and Kang G Shin. 2019. Spatio-temporal capsule-based reinforcement learning for mobility-on-demand network coordination. In *Proc. WWW*. 2806–2813.
- [11] Suining He and Kang G Shin. 2020. Dynamic Flow Distribution Prediction for Urban Dockless E-Scooter Sharing Reconfiguration. In *Proc. WWW*. 133–143.
- [12] Suining He and Kang G Shin. 2020. Towards Fine-grained Flow Forecasting: A Graph Attention Approach for Bike Sharing Systems. In *Proc. WWW*. 88–98.
- [13] Wenhao Huang, Guojie Song, Haikun Hong, and Kunqing Xie. 2014. Deep architecture for traffic flow prediction: deep belief networks with multitask learning. *IEEE T-ITS* 15, 5 (2014), 2191–2201.
- [14] Pierre Hulot, Daniel Aloise, and Sanjay Dominik Jena. 2018. Towards station-level demand prediction for effective rebalancing in bike-sharing systems. In *Proc. ACM KDD*. 378–386.
- [15] Abhinav Jauhri, Brian Foo, Jerome Berclaz, Chih Chi Hu, Radek Grzeszczuk, Vasu Parameswaran, and John Paul Shen. 2017. Space-time graph modeling of ride requests based on real-world data. In *Proc. AAAI*.
- [16] Yexin Li, Yu Zheng, Huichu Zhang, and Lei Chen. 2015. Traffic prediction in a bike-sharing system. In *Proc. ACM SIGSPATIAL*. 33.
- [17] Youru Li, Zhenfeng Zhu, Deqiang Kong, Meixiang Xu, and Yao Zhao. 2019. Learning Heterogeneous Spatial-Temporal Representation for Bike-Sharing Demand Prediction. In *Proc. AAAI*, Vol. 33. 1004–1011.
- [18] Tsungnan Lin, Bill G Horne, Peter Tino, and C Lee Giles. 1996. Learning long-term dependencies in NARX recurrent neural networks. *IEEE TNNLS* 7, 6 (1996), 1329–1338.
- [19] Junming Liu, Qiao Li, Meng Qu, Weiwei Chen, Jingyuan Yang, Hui Xiong, Hao Zhong, and Yanjie Fu. 2015. Station site optimization in bike sharing systems. In *Proc. IEEE ICDM*. IEEE, 883–888.
- [20] Junming Liu, Leilei Sun, Weiwei Chen, and Hui Xiong. 2016. Rebalancing bike sharing systems: A multi-source data smart optimization. In *Proc. ACM KDD*. 1005–1014.
- [21] Junming Liu, Leilei Sun, Qiao Li, Jingci Ming, Yanchi Liu, and Hui Xiong. 2017. Functional zone based hierarchical demand prediction for bike system expansion. In *Proc. ACM SIGKDD*. 957–966.
- [22] Zhaoyang Liu, Yanyan Shen, and Yanmin Zhu. 2018. Inferring dockless shared bike distribution in new cities. In *Proc. ACM WDSM*. 378–386.
- [23] Zhaoyang Liu, Yanyan Shen, and Yanmin Zhu. 2018. Where Will Dockless Shared Bikes be Stacked? —Parking Hotspots Detection in a New City. In *Proc. ACM KDD*. 566–575.
- [24] Yisheng Lv, Yanjie Duan, Wenwen Kang, Zhengxi Li, and Fei-Yue Wang. 2014. Traffic flow prediction with big data: a deep learning approach. *IEEE T-ITS* 16, 2 (2014), 865–873.
- [25] Xiaolei Ma, Zhuang Dai, Zhengbing He, Jihui Ma, Yong Wang, and Yunpeng Wang. 2017. Learning traffic as images: a deep convolutional neural network for large-scale transportation network speed prediction. *Sensors* 17, 4 (2017), 818.
- [26] Eoin O'Mahony and David B Shmoys. 2015. Data analysis and optimization for (Citi)bike sharing. In *Proc. AAAI*.
- [27] Ling Pan, Qingpeng Cai, Zhixuan Fang, Pingzhong Tang, and Longbo Huang. 2019. A deep reinforcement learning framework for rebalancing dockless bike sharing systems. In *Proc. AAAI*, Vol. 33. 1393–1400.
- [28] Yan Pan, Ray Chen Zheng, Jiayi Zhang, and Xin Yao. 2019. Predicting bike sharing demand using recurrent neural networks. *Procedia Computer Science* 147 (2019), 562–566.
- [29] Zheyi Pan, Yuxuan Liang, Weifeng Wang, Yong Yu, Yu Zheng, and Junbo Zhang. 2019. Urban traffic prediction from spatio-temporal data using deep meta learning. In *Proc. ACM KDD*. 1720–1730.
- [30] Xianfeng Tang, Boqing Gong, Yanwei Yu, Huaxiu Yao, Yandong Li, Haiyong Xie, and Xiaoyu Wang. 2019. Joint modeling of dense and incomplete trajectories for citywide traffic volume inference. In *Proc. WWW*. 1806–1817.
- [31] Shuai Wang, Tian He, Desheng Zhang, Yuanhao Shu, Yunhui Liu, Yu Gu, Cong Liu, Haengju Lee, and Sang H Son. 2018. BRAVO: Improving the rebalancing operation in bike sharing with rebalancing range prediction. *Proc. ACM IMWUT* 2, 1 (2018), 1–22.
- [32] Huaxiu Yao, Yiding Liu, Ying Wei, Xianfeng Tang, and Zhenhui Li. 2019. Learning from multiple cities: A meta-learning approach for spatial-temporal prediction. In *Proc. WWW*. 2181–2191.
- [33] Bing Yu, Haoteng Yin, and Zhanxing Zhu. 2017. Spatio-temporal graph convolutional networks: A deep learning framework for traffic forecasting. *arXiv preprint arXiv:1709.04875* (2017).
- [34] Jiawei Zhang, Xiao Pan, Moyin Li, and Philip S Yu. 2016. Bicycle-sharing systems expansion: station re-deployment through crowd planning. In *Proc. ACM SIGSPATIAL*. 1–10.
- [35] Jiawei Zhang and S Yu Philip. 2016. Trip route planning for bicycle-sharing systems. In *Proc. IEEE CIC*. IEEE, 381–390.
- [36] Xiaolu Zhou. 2015. Understanding spatiotemporal patterns of biking behavior by analyzing massive bike sharing data in Chicago. *PLoS One* 10, 10 (2015), e0137922.